

FIRST HIGH CONTRAST IMAGING USING A GAUSSIAN APERTURE PUPIL MASK

JOHN H. DEBES¹, JIAN GE

AND

ABHIJIT CHAKRABORTY

Pennsylvania State University

Department of Astronomy & Astrophysics, University Park, PA 16802, USA

Draft version October 27, 2018

ABSTRACT

Placing a pupil mask with a gaussian aperture into the optical train of current telescopes represents a way to attain high contrast imaging that potentially improves contrast by orders of magnitude compared to current techniques. We present here the first observations ever using a gaussian aperture pupil mask (GAPM) on the Penn State near-IR Imager and Spectrograph (PIRIS) at the Mt. Wilson 100" telescope. Two nearby stars were observed, ϵ Eridani and μ Her A. A faint companion was detected around μ Her A, confirming it as a proper motion companion. Furthermore, the observed H and K magnitudes of the companion were used to constrain its nature. No companions or faint structure were observed for ϵ Eridani. We found that our observations with the GAPM achieved contrast levels similar to our coronagraphic images, without blocking light from the central star. The mask's performance also nearly reached sensitivities reported for other ground based adaptive optics coronagraphs and deep HST images, but did not reach theoretically predicted contrast levels. We outline ways that could improve the performance of the GAPM by an order of magnitude or more.

Subject headings: binaries:close—instrumentation:miscellaneous—stars:individual(ϵ Eridani, HD 161797)—stars:low mass

1. INTRODUCTION

The search to directly image an extrasolar Jovian planet requires contrast levels of $\sim 10^{-9}$ a few λ/D from the central star. Scattered light in a telescope and the diffraction pattern of the telescope's aperture limit the contrast possible for direct detection of faint companions. The circular aperture of telescopes creates a sub-optimal diffraction pattern, the so-called Airy Pattern which is azimuthally symmetric. In addition, the intensity in the diffraction pattern of the circular aperture declines as θ^{-3} . Currently the best way to diminish the Airy pattern is to use a coronagraph by using the combination of a stop in the focal plane that rejects a majority of the central bright object's light and a Lyot stop in the pupil plane to reject high frequency light (Lyot 1939; Malbet 1996; Sivaramakrishnan et al. 2001). Several recent ideas explore the use of alternative "apodized" apertures for high contrast imaging in the optical or near-infrared (Nisenson & Papaliolios 2001; Spergel 2001; Ge & Debes 2002). These ideas revisit ideas first experimented with in the field of optics (Jacquinot & Roizen-Dossier 1964, and references therein).

Apodizing an aperture rather than creating new technology to null or block a central bright object's light has several advantages. Alignment of an object with an apodized aperture is not necessary, whereas for nulling interferometry or coronagraphy it is essential. The cost of creating a shaped aperture is also quite low, if one makes the apodized aperture shape as a pupil mask in the optical train. This allows any current telescope to easily perform high contrast imaging. Each telescope would then take images where the contrast would be only limited by at-

mospheric turbulence and scattered light in the optical system.

A promising design for a shaped aperture was recently suggested by Spergel (2001). In this case the top and bottom edges of the aperture are described by gaussian functions:

$$y_t = aR \left\{ \exp \left[-(\alpha x/R)^2 \right] - \exp(-\alpha^2) \right\} \quad (1)$$

$$y_b = -bR \left\{ \exp \left[-(\alpha x/R)^2 \right] - \exp(-\alpha^2) \right\} \quad (2)$$

where x goes from $-R < x < R$. The fourier transform of the aperture shape function gives the resulting diffraction pattern in the imaging plane. Since the fourier transform of a gaussian is another gaussian, the intensity of the diffraction pattern along one image plane axis decreases exponentially, which we denote the high contrast axis. The variables a , b , and α are all free parameters that can be used to optimize the aperture for depth of contrast, the angle from the central object at which high contrast starts, and the azimuthal area of high contrast.

In order to test the performance of a gaussian aperture pupil mask on a telescope we designed a cold gaussian pupil mask and placed it in the optical train of the Penn State near-IR Imager and Spectrograph (PIRIS) for near-infrared imaging (Ge et al. 2001; Ge & Debes 2002). Figure 1 shows our pupil mask design. The placement of gaussian apertures avoided the support structure of the telescope to maximize contrast at the cost of halving the resolution of the images. Throughput was also an issue, so to achieve roughly 25% throughput a total of 12 apertures were situated symmetrically in each quadrant of the pupil mask. To maximize the azimuthal coverage so that

¹ NASA GSRP Fellow, debes@astro.psu.edu

in any one image roughly half of the azimuthal area was in a high contrast region, we varied the height of the top and bottom of the apertures. Full details of our design will be published in a future paper (Debes & Ge 2002, in preparation). The current pupil design would be well suited for existing 10m telescopes to look for faint companions separated from their parent stars by 5 AU out to ~ 40 pc in the visible or ~ 10 pc for the near-IR limited only by atmospheric turbulence and scattered light in the telescope. Scattered light is not a hard limit; with a deformable mirror dedicated to correcting mirror surface errors, the levels of scattered light can be reduced by ~ 1 -2 orders of magnitude (Malbet, Yu, & Shao 1995).

We report here the first results of observations using the GAPM to demonstrate the feasibility of using such a mask at an observatory. While the testing of optics with a GAPM has been mentioned before (Jacquinot & Roizen-Dossier 1964, e.g.), to our knowledge these are the first astronomical observations using a GAPM for detecting faint companions. In Section 2 we will describe the observations we have done to date, and in Section 3 we present our results. Finally, in Section 4 we discuss the implications of our results.

2. OBSERVATIONS

The stars ϵ Eridani (GJ 144 = HD 22049 = HR 1084, $V=3.72$, $d=3.2$ pc) and μ Her A (GJ 695A = HD 161797 = HR 6623, $V=3.41$, $d=8.4$ pc) were observed with the GAPM. The star ϵ Eridani was observed with seven 4s integrations in the K band, while μ Her A was observed with one 3s and one 10s integration in the H band. Both objects were also observed in normal imaging modes. The plate scale and orientation for PIRIS was determined by measuring the positions of several stars in the Orion Nebula and comparing them to 2MASS data. We find that the plate scale of PIRIS is $.082'' \pm .001'' \text{ pixel}^{-1}$.

The GAPM was aligned 23° clockwise from North to line up with the support structure of the telescope. Therefore, the axis of greatest contrast would be oriented perpendicular to the alignment of the mask or along a line running from the NW to the SE in an image.

For our coronagraphic modes we used a stop in the focal plane that has a gaussian transmission function (Nakajima 1994) with a fwhm of $\sim 1''$ in an image. A Lyot stop was placed in the pupil plane whose dimensions were chosen for an optimal combination of throughput and contrast (Ge & Debes 2002; Ftaclas 2001, private communication).

3. RESULTS

3.1. ϵ Eridani

Figure 2 shows a logarithmic scaled image of the PSF of the GAPM rotated so that the high contrast area is horizontal. The PSF of the GAPM is not azimuthally symmetric and the high contrast region extends roughly over 180° . The majority of light in the diffraction pattern is spread into the four wings, leaving higher contrast regions between them. For comparison, an image of the theoretical PSF of the GAPM is pictured. No faint companions were detected, but fairly stringent limits can be imposed on what kind of companions would have been detected between $1''$ and $10''$ from the central star in the high contrast regions.

In order to test the level of contrast achieved by the gaussian mask in comparison to other modes of PIRIS, coronagraphic and adaptive optics observations were taken of the star+faint companion system G1 105 (Golimowski et al. 1995, 2000). Figure 3 shows the differences in the three modes plus a simulation of the performance of our pupil mask design with no scattered light or atmospheric turbulence. The observations were azimuthally averaged in high contrast areas. For G1 105, we azimuthally averaged the PSF with the exception of 35° on either side of the faint companion. The resulting profiles were then normalized to peak flux. Further scaling had to be performed for the coronagraphic and gaussian pupil mask profiles. In these two cases the peak flux could not be determined due to the coronagraphic mask for G1 105 and due to saturation for ϵ Eridani. In the case of G1 105 this problem was circumvented by the presence of the companion which was used to properly scale the flux. The error in the curve for the coronagraph is due mostly to uncertainties in the positions and flux ratio of the companion and the central star, but should be no larger than on the order of 10%. In the case of ϵ Eridani we took unsaturated images of a dimmer standard star and normalized the azimuthally averaged PSF at $.82''$. The profile of the GAPM is a composite of those two sets of observations. The error in this normalization is dominated by variations in the PSF and to estimate the effects of this we varied the point at which we normalized the two profiles. We found that at most the error introduced is of the order 25%.

As can be seen in Figure 3, the GAPM performs better than AO alone and is ~ 2 times worse than a traditional coronagraph $> 1''$. This is without any attempt to block the light of the central star. We discuss avenues for improving the performance of the mask in Section 4. Comparison of normalized contrast versus λ/D to other coronagraphs and to deep HST WFPC2 observations of ϵ Eridani show that our gaussian pupil and coronagraphic mode performs similarly in terms of contrast to previous work done (Schroeder et al. 2000; Hayward et al. 2001; Luhman & Jayawardhana 2002). It is also evident that several effects degrade contrast severely from the theoretical simulation. A large part of this degradation is due to the scattered light in the telescope and the AO. We discuss the possible causes of contrast degradation in Section 4.

From the azimuthally averaged profiles, limits to the type of companions we could have detected around ϵ Eridani can be estimated. Beyond $4''$ (~ 13 AU), any companion with $\Delta m_K < 9.3$ mag would have been detected, and at $8''$ (~ 26 AU) any companion < 11.8 mag would have been detected. These translate to M_K of 13.6 and 16.1 respectively. Age is also an important consideration when talking about faint companions. The age of ϵ Eridani is not well known, but should be < 1 Gyr (Soderblom & Dappen 1989; Drake & Smith 1993). A more recent evaluation on the data for ϵ Eridani places the age at $.73 \pm .2$ Gyr (Song et al. 2000). We looked at the models of Burrows et al. (1997) and Chabrier et al. (2000) to determine the range of possible companion masses that we could have detected based on $.7$ Gyr and $M_K=13.6$ and 16.1 , corresponding to $38 \pm 8 M_J$ and $20 \pm 5 M_J$. We derived these estimates by taking a value intermediate to the two models, while the error represents their spread.

3.2. μ Her A

A faint companion around μ Her A was detected with high S/N in both GAPM and AO images. Fig 4 shows the raw H image which clearly shows the faint companion. This companion was previously detected in R and I band AO images at Mt. Wilson, and used to explain a radial velocity acceleration corresponding to a ~ 30 yr orbit (Turner et al. 2001; Cumming, Marcy, & Butler 1999; Cochran & Hatzes 1994). Measurements of the separation from AO images were complicated by the saturation of μ Her A, but the center position was calculated by fitting a gaussian profile horizontally and vertically to unsaturated parts of the PSF. We measured the separation of the companion to be $1.''3 \pm .''2$ (~ 11 AU) with a P.A. of $184^\circ \pm 8^\circ$. Errors represent $2\text{-}\sigma$. These measurements are consistent with those reported by Turner et al. (2001), although we measure a change in P.A. of $\sim 17^\circ$. The proper motion of μ Her A is -291.42 mas/yr in right ascension and -750.03 mas/yr in declination, which implies that a much larger change in separation would have been detected had the two objects not been bound (Perryman et al. 1997). Our observations confirm the dimmer object to be a proper motion companion and thus physically bound to the brighter star.

The nature of the companion has previously been suggested to be substellar from Monte Carlo calculations of probable mass based on observed angular separation (Torres 1999). However, the observed photometry of the companion and the age of the primary star do not support that conclusion. Unfortunately, standard star measurements with the GAPM could not be performed, but we took H and K photometry with the normal imaging mode of PIRIS. We find that for the companion $m_H=8.5 \pm .1$ and $m_K=7.9 \pm .1$, which corresponds to $M_H=8.9$ and $M_K=8.3$. The age of μ Her A has been estimated to be 10.6 Gyr by measurements of its magnetic activity (Barry, Cromwell, & Hege 1987). However, there is a dependence on such measurements based on the $[\text{Fe}/\text{H}]$ of the star. Using Rocha-Pinto & Maciel (1998)'s correction for metallicity and $[\text{Fe}/\text{H}]=.15$ from Cayrel de Strobel (1981) gives a corrected age of 4.2 Gyr. Turner et al. (2001) reports a $\Delta m_R=9.29$ and $\Delta m_I=7.26$ between μ Her A and its faint companion. Taking the observed m_R and m_I of the central star from Johnson et al. (1966) one derives for the faint companion $m_R=12.18$ and $m_I=9.77$, corresponding to $M_R=12.6$ and $M_I=10.2$. Along with the age, M_R , M_I , M_H , and M_K of the companion, we used the models of Baraffe et al. (1998, 2002) to conclude that its mass should be $\sim .13 M_\odot$. It should be noted that at this mass the R and I band is anomalously bright by .4 and 1.2 mag respectively, while both H and K observations match the models to within the errors. Baraffe et al. (1998) mentions that the opacity around $1\mu\text{m}$ is not well known and when compared to observations, the models appear to overestimate the opacity in the R band, while underestimating opacity around the V band. In order to test this hypothesis Baraffe et al. (1998) arbitrarily increased the opacity in the V band and found an increase in flux in the I band. At the same time this uncertainty had little effect on the JHK bands. We therefore regard the H and K magnitudes to be a more reliable photometric indicator. Even if the R and I magnitudes are a better measurement to compare to models, the companion is above the hydrogen burning limit. Spectra

of the companion would be valuable in definitively settling its identity. Such transition objects are extremely useful for constraining low mass stellar models as well as determining the low mass end of the star formation rate.

4. DISCUSSION

These observations represent the first attempt at high contrast imaging with a GAPM. The relative ease and speed with which these first masks have been produced and their performance presents a promising technology that when mature may provide a viable alternative to coronagraphy as a high contrast imaging mode. The fact that this preliminary attempt achieves contrasts similar to modern techniques in coronagraphy while not blocking any of the central star's light is significant and encouraging for both ground based and space based attempts to directly image extrasolar planets. Several factors have degraded the performance of the mask from reaching its theoretical sensitivities.

Our theoretical treatment of the mask neglects imperfect atmospheric correction, scattered light in the telescope, and the presence of a thermal background, all of which contribute to degrading the performance of the mask. Images of the pupil plane (including the gaussian mask) show the presence of a small diffuse thermal background in the areas that have been blocked and should not emit light, on the order of 1% the peak flux coming through the gaussian openings. Similarly, diffraction at the smallest openings of the gaussian aperture may wash out the gaussian shape and also significantly degrade contrast. Perhaps the most significant degradation comes from the imperfect correction of the atmosphere in the AO system. All of these factors must be quantified fully, which will be explored in a forthcoming paper (Debes & Ge 2002, in preparation).

There are several ways to drastically improve the performance of the GAPM. Suppression of any thermal background, widening the opening of the aperture to reduce diffraction effects, and higher precision construction of the masks all are relatively quick ways to increase performance. Additionally the GAPM should be able to be combined with a coronagraphic mask in the focal plane. Based on the performance of our coronagraphic modes that can suppress the light from the central star by about an order of magnitude, we would expect our GAPM and coronagraphic mask to achieve sensitivities ~ 5 times better than the coronagraphic mask and Lyot stop. Longer term goals would be to design telescopes and instruments optimized for the suppression of excess scattered light and aberrations.

We thank D. McCarthy for loaning part of the optics for PIRIS, R. Brown for the PICNIC array, C. Ftacilas for coronagraphic masks, and A. Kutyrev for filters. Several important discussions with D. Spergel were crucial in our understanding of gaussian apertures. We would also like to thank the invaluable help of the Mt. Wilson staff and L. Engel for design help with the GAPM.

J.D acknowledges funding by a NASA GSRP fellowship under grant NGT5-119. This work was supported by NASA with grants NAG5-10617, NAG5-11427 as well as the Penn State Eberly College of Science.

REFERENCES

- Baraffe, I. et al. 1998, *A&A*, 337, 403.
Baraffe, I. et al. 2002, *A&A*, 382, 563.
Barry, D. C., Cromwell, R. H., & Hege, E. K. 1987, *ApJ*, 315, 264.
Burrows, A. et al. 1997, *ApJ*, 491, 856.
Cayrel de Strobel, G. 1981, *BICDS*, 20, 28.
Chabrier, G. et al. 2000, *ApJ*, 542, 464.
Cochran, W. D. & Hatzes, A. P. 1994, *Ap&SS*, 212, 281.
Cumming, A., Marcy, G. W., & Butler, R. P. 1999, *ApJ*, 526, 890.
Drake, J. J. & Smith, G. 1993, *ApJ*, 412, 797.
Ge, J. et al. 2001, *AAS*, 199, 3304.
Ge, J. & Debes, J. H. 2002, *SPIE*, (in press)
Golimowski, D. A. et al. 2000, *AJ*, 120, 2082.
Golimowski, D. A. et al. 1995, *ApJ*, 452, L125.
Jacquinot, P. & Roizen-Dossier, B. 1964, *Progress In Optics*, 3, 31.
Johnson, H. L. et al. 1966, *CLPL*, 4, 99.
Hayward, T. L. et al. 2001, *PASP*, 113, 105.
Song, I. et al. 2000, *ApJ*, 533, L41.
Luhman, K. L. & Jayawardhana, R. 2002, *ApJ*, 566, 1132.
Lyot, B. 1939, *MNRAS*, 99, 580.
Malbet, F. 1996, *A&AS*, 115, 161.
Malbet, F., Yu, J. W., & Shao, M. 1995, *PASP*, 107, 386.
Nakajima, T. 1994, *ApJ*, 425, 348.
Nisenson, P. & Papaliolios, C. 2001, *ApJ*, 548, L201.
Perryman, M. A. C. et al. 1997, *A&A*, 323, L49.
Rocha-Pinto, H. J. & Maciel, W. J. 1998, *MNRAS*, 298, 332.
Schroeder, D. J. et al. 2000, *AJ*, 119, 906.
Sivaramakrishnan, A. et al. 2001, *ApJ*, 552, 397.
Soderblom, D. R. & Dappen, W. 1989, *ApJ*, 342, 945.
Spergel, D. N. 2001, preprint(astro-ph/0101142)
Turner, N. H. et al. 2001, *AJ*, 121, 3254.
Torres, G. 1999, *PASP*, 111, 169.

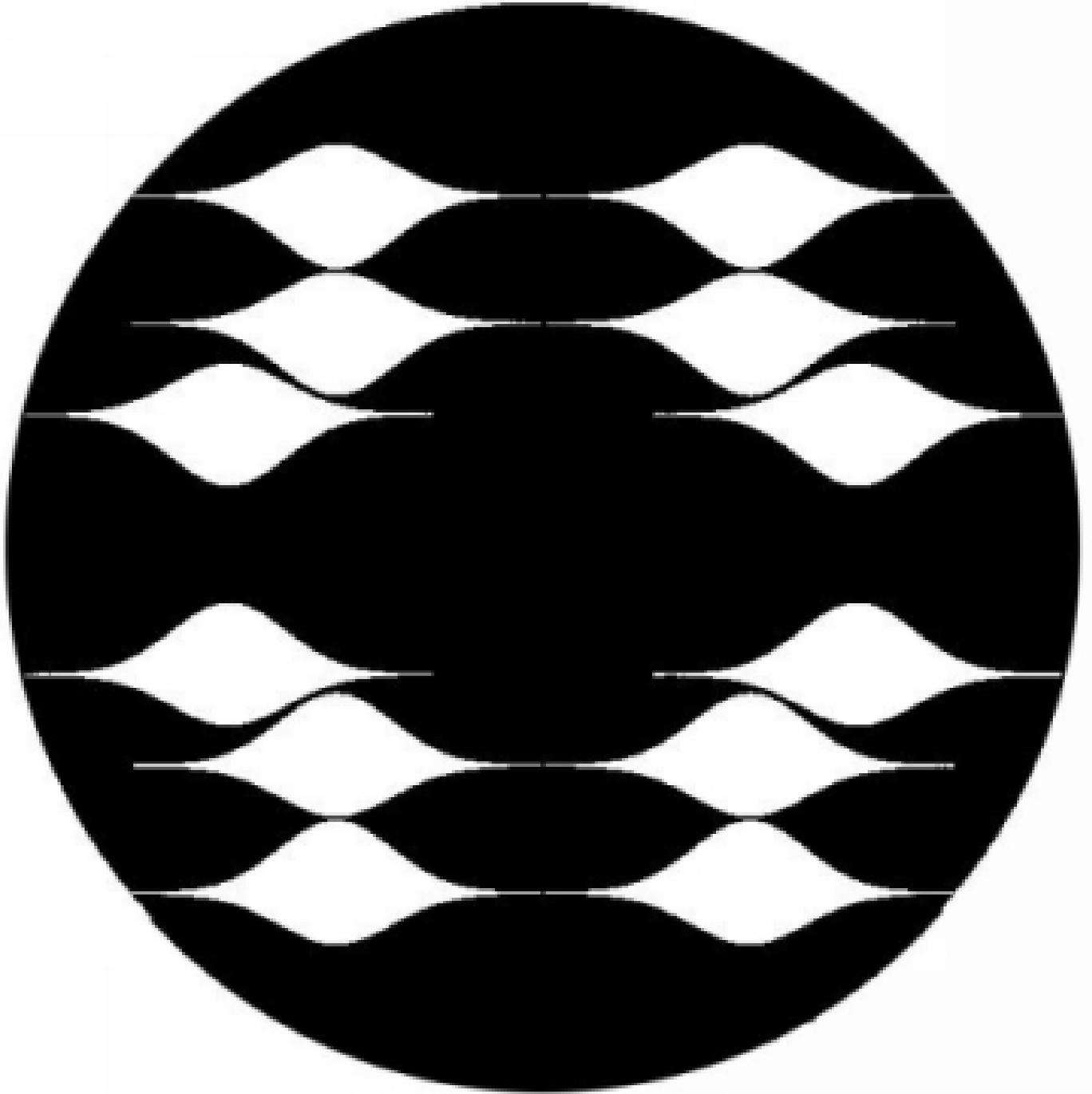


FIG. 1.— Design of the GAPM used at Mt. Wilson. Twelve apertures were used to provide throughput and avoid the support structure of the telescope.

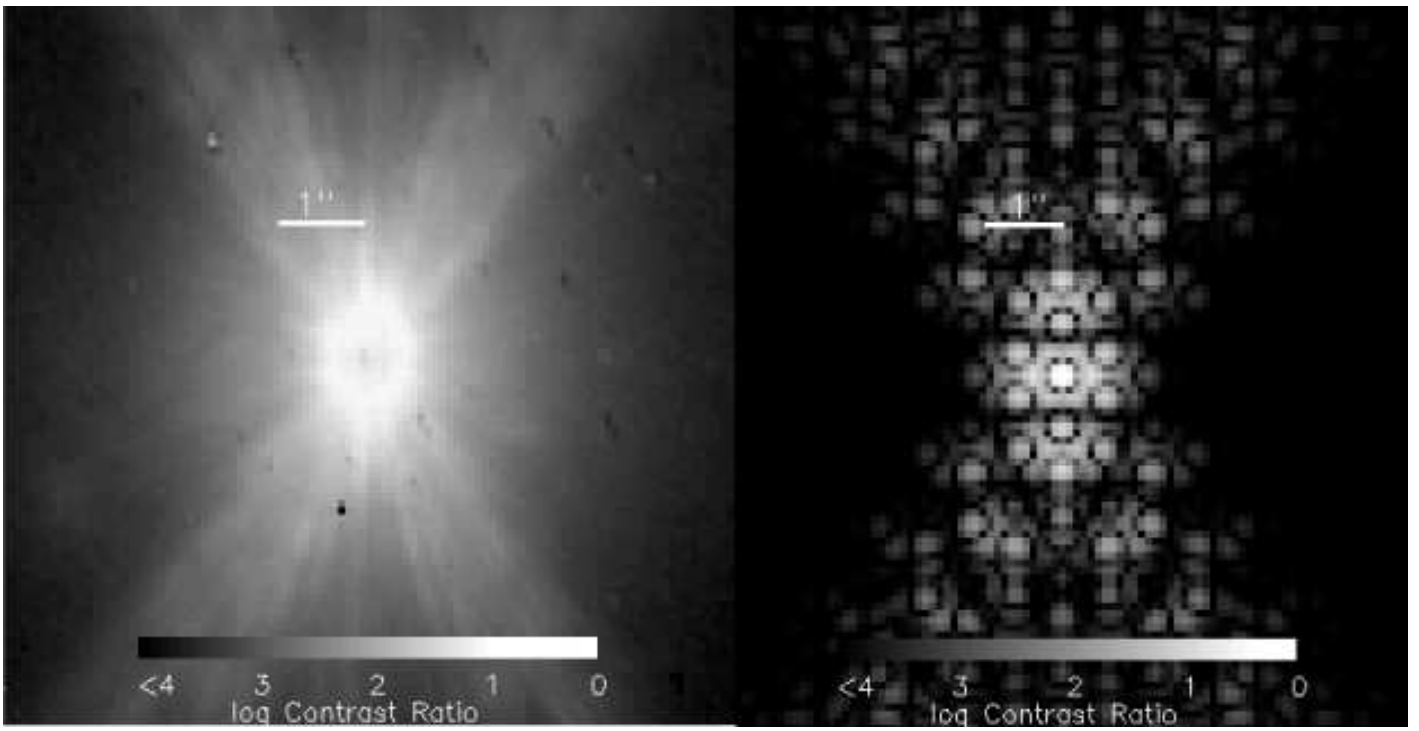


FIG. 2.— Co-added image of ϵ Eridani with a GAPM, the first observations ever done. The right image shows a theoretically produced PSF for comparison. The scale for the image is logarithmic to show high contrast features.

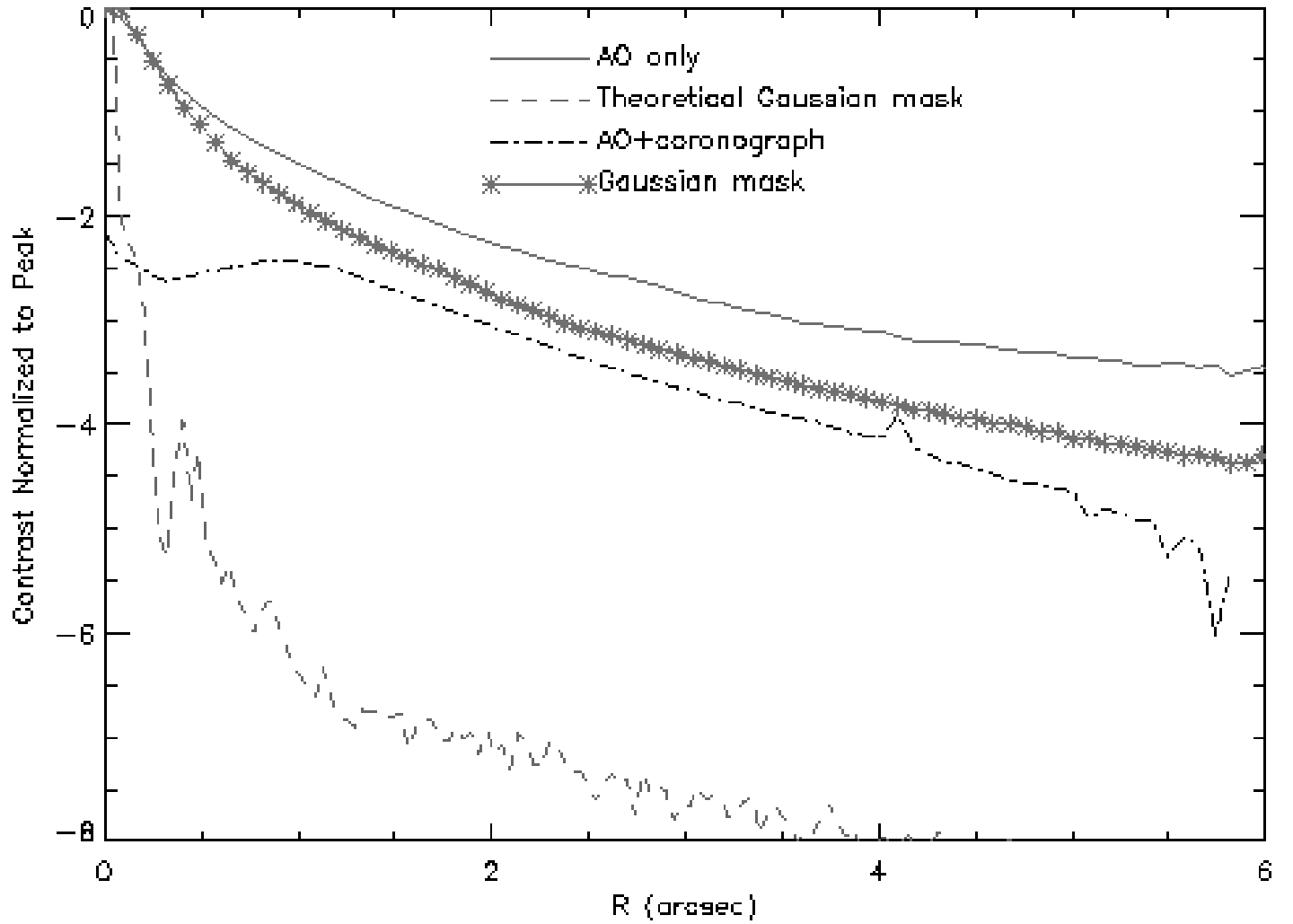


FIG. 3.— Comparisons of contrast achieved with the GAPM and other modes of PIRIS. The GAPM performs only a factor of two worse than a traditional coronagraph without blocking any of the central star's light.

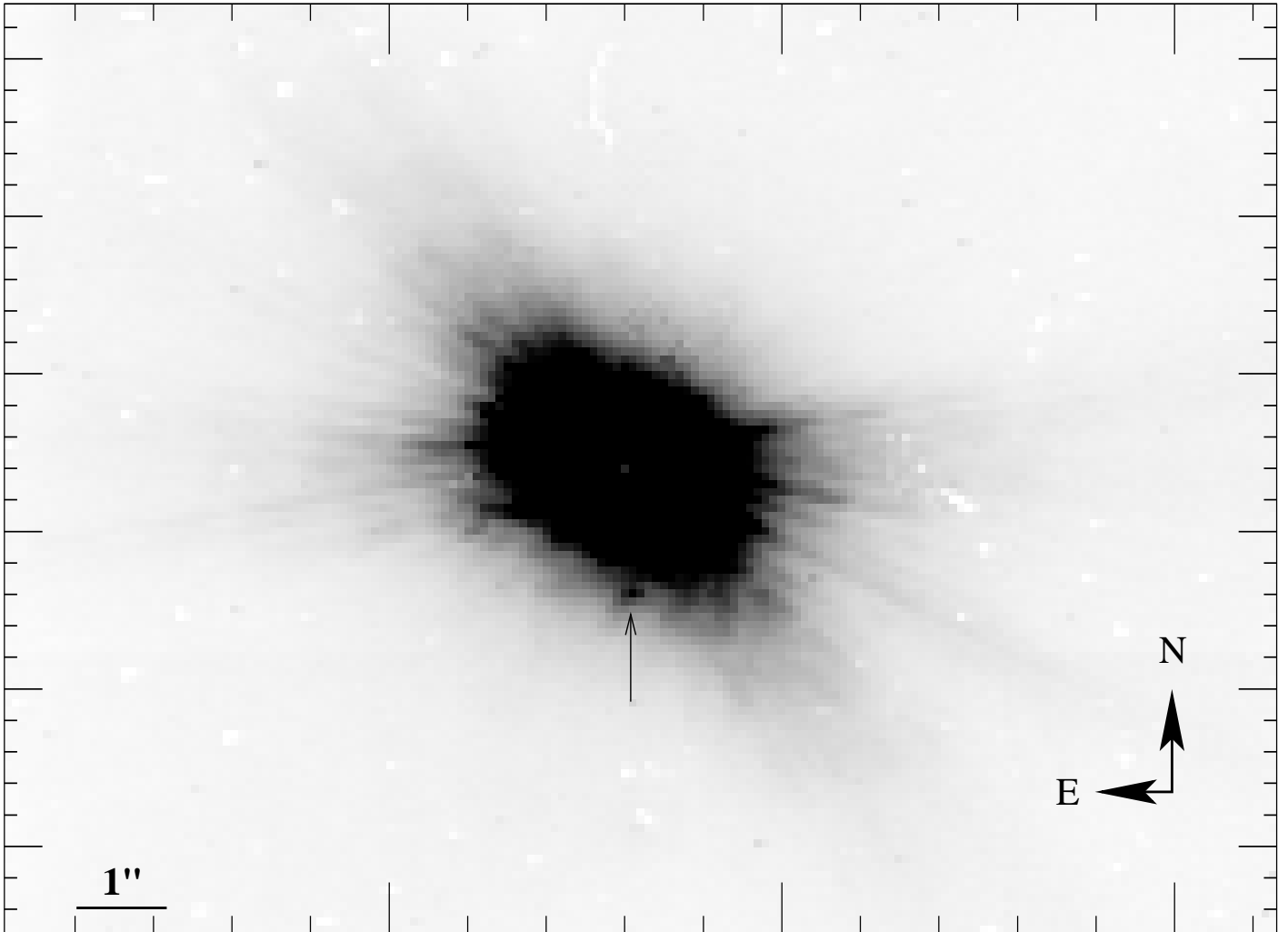


FIG. 4.— Raw image of μ Her A and its faint companion taken with the GAPM. The companion is clearly visible, and confirms it as a proper motion companion to μ Her A.